Neural Computing and Applications (2024) 36:18151–18159
https://doi.org/10.1007/s00521-024-10050-3

ORIGINAL ARTICLE

Chimera states and information transfer in interacting populations of map-based neurons

V. J. Márquez-Rodríguez[1,2] · K. Tucci[2] · M. G. Cosenza[3]

Received: 31 December 2023 / Accepted: 19 June 2024 / Published online: 19 July 2024

Abstract
We investigate the synchronization behavior and the emergence of chimera states in a system of two interacting populations of maps possessing chaotic neural-like dynamics. We characterize four collective states on the space of coupling parameters of the system: complete synchronization, generalized synchronization, chimera states, and incoherence. We quantify the information exchange between the two neuron populations in chimera states. We have found a well-defined direction of the flow of information in chimera states, from the desynchronized population to the synchronized one. The incoherent population functions as a driver of the coherent neuron population in a chimera state. This feature is independent of the population sizes or population partitions. Our results yield insight into the communication mechanisms arising in brain processes such as unihemispheric sleep and epileptic seizures that have been associated to chimera states.

Keywords Chimera states · Information transfer · Coupled map networks · Neural dynamics · Chaos synchronization

1 Introduction

The study of emergent collective states in systems composed of interacting populations of dynamical units is a relevant topic in complexity science. These systems have been investigated in many different areas, such as coupled networks of oscillators [1, 2], cohabitation of two biological species [3, 4], competition of two languages [5], and neural networks [6, 7]. In the context of neural systems, the study of interacting populations of dynamical units can be relevant to understand the functional dynamics of the brain [8, 9]. Two population models have been used in several studies, such as synchronization between oscillations emerging from separated cortical neuronal assemblies [10], neuronal information processing [11], and phase-coherence transitions between delay-coupled neuronal populations [12].

In many systems, collective behavior can be characterized as synchronization states arising from the interactions within and between populations. Recently, there has been great interest in the study of chimera states in dynamical networks [13–16]. A chimera state consists of the coexistence of subsets of elements with synchronous and asynchronous dynamics in a spatiotemporal system. In a system of two interacting populations, a chimera state is manifested as one population displaying a synchronized behavior while the other remains desynchronized. Chimera states have been found in systems consisting of two interacting populations of oscillators [2, 17–20] and in cross-cultural interactions of two social groups [21]. They have been experimentally observed in two coupled populations of mechanical oscillators [22] and electrochemical oscillators [23].

✉ V. J. Márquez-Rodríguez
jmarquezr@udd.cl

K. Tucci
ktucci@gmail.com

M. G. Cosenza
mcosenza@yachaytech.edu.ec

[1] Laboratorio de Neurociencia Social y Neuromodulación, Centro de Investigación en Complejidad Social (neuroCICS), Facultad de Gobierno, Universidad del Desarrollo, Avenida Las Condes, 12461, Santiago 7550000, Chile

[2] Facultad de Ciencias, SUMA-CeSiMo, Universidad de Los Andes, Av.Alberto Carnevalli, Mérida 5101, Venezuela

[3] Grupo Interdisciplinario de Sistemas Complejos, Escuela de Ciencias Físicas y Nanotecnología, Universidad Yachay Tech, Urcuquí, Ecuador

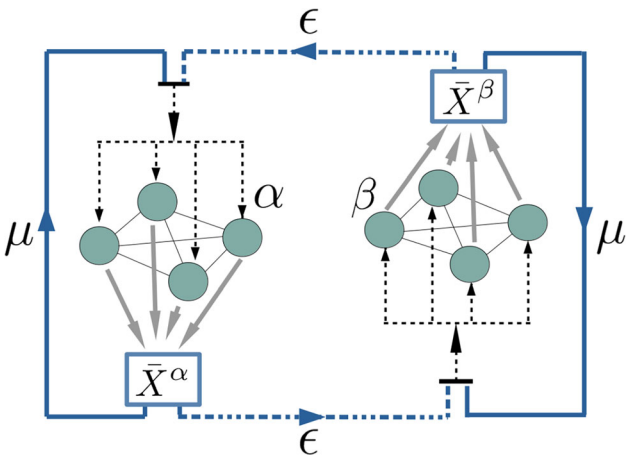

Fig. 1 Scheme of two populations α and β reciprocally interacting through their mean fields. Any element in population $\alpha[\beta]$ interacts with: (i) all other elements in $\alpha[\beta]$ through the mean field $\bar{X}^{\alpha}$ $[\bar{X}^{\beta}]$ with coupling parameter μ, and (ii) the mean field $\bar{X}^{\beta}$ $[\bar{X}^{\alpha}]$ of population $\beta[\alpha]$ with strength ϵ

Chimera states have been associated to brain processes such as unihemispheric sleep in various animal species including birds, aquatic mammals, and reptiles [24, 25], as well as human electroencephalographic patterns in epileptic seizures [26, 27]. Chimera states have been found in a two-layer network brain model based on data from cerebral cortex [28] and in two-layer neuronal network with unidirectional inter-layer links [29]. Chimeras in neural systems have been mostly studied in models of coupled differential equations, such as the Hodgkin–Huxley model [30], the Hindmarsh–Rose model [31–33], and the Fitzhugh–Nagumo model [34, 35]. More recently, chimera states have been reported in networks with neural-type local dynamics described by the Rulkov time-discrete map [36, 37].

In many situations, it is important not only to characterize chimeras or other collective states, but also to understand the causal relationships between the constituent parts of a system that leads to such behaviors. In particular, information transfer measures have been proven useful to quantify drive–response causal relationships between subsystems and functional structures in diverse complex systems [38]. For example, the emergence of nontrivial collective behavior in chaotic dynamical networks has been associated to the flow of information from global to local scales [39]. Transfer entropy methods have been widely employed in neuroscience to evaluate interdependence between electroencephalographic data sets [40]. Such measures allow, for instance, to evaluate coupling directions [41] and connectivity [42] between different regions of the brain.

In this article, we investigate the emergence of synchronization and chimera states in a system of two interacting populations of chaotic maps possessing neural-like dynamics. We characterize various synchronization states that arise in the system: complete synchronization, generalized synchronization, chimera states, and incoherence. Specifically, we address the question: who is the driver in a chimera state in neuron dynamical networks? We quantify the information flow between the synchronized and desynchronized neuron populations in a chimera state by employing the information transfer measure of Schreiber [43] in order to gain insight into the communication mechanisms associated to pathologies in the brain. We compare the information transfer between the mean fields of the two populations in chimera states. Our approach is simpler than methods based on delayed mutual information and Poincaré sections used to detect the flow of information in chimera states of phase oscillator networks [44].

In Sect. 2, we introduce a model of two populations interacting through their mean fields and define the order parameters to characterize synchronization states. Section 3 describes the spatiotemporal patterns associated to the different collective synchronization states arising in the system. The collective states are characterized on the phase space given by the coupling parameters of the system. Section 4 contains the calculation of the information transfer between the two neuron populations in a chimera state. We find a definitive direction of the flow of information from the desynchronized population to the synchronized one. Conclusions are presented in Sect. 5.

2 Model for two interacting populations of map-based neurons

Coupled map lattices or coupled map networks are spatiotemporal dynamical systems where space and time are discrete, but the state variables are continuous. They consist of a set of maps or iterative functions considered as nodes interacting on a lattice or network [45, 46]. Coupled map networks have provided useful models for the study of diverse processes in spatially extended systems, with the advantage of being computationally efficient [47]. The discrete-space character of coupled map systems makes them appropriate for the investigation of dynamics on nonuniform networks [48].

Our system is composed of N maps possessing neuron dynamics, distributed into two populations denominated as α and β, with sizes N^{α} and N^{β}, respectively, such that $N = N^{\alpha} + N^{\beta}$. In order to model local excitable dynamics, we consider two-dimensional map-based neurons where the two variables may represent the membrane potential and outward ionic currents, respectively. We use the

notation $[k]$ to indicate "or k." Then, the state of element $i[j] \in \alpha[\beta]$ at discrete time t is given by two variables $x_t^{\alpha}(i), y_t^{\alpha}(i)$ $[x_t^{\beta}(j), y_t^{\beta}(j)]$, where $i = 1, 2, \ldots, N^{\alpha}$ and $j = 1, 2, \ldots, N^{\beta}$. We assume that each element within a population interacts with the mean field of that population and with the mean field of the other population. Mean-field coupling has been used in neural mass models [6, 49, 50]. Then, we define the dynamics of the two interacting populations of map-based neurons by the following coupled map equations,

$$x_{t+1}^{\alpha}(i) = (1-\mu) f(x_t^{\alpha}(i), y_t^{\alpha}(i)) + \mu \bar{X}_t^{\alpha} + \epsilon \bar{X}_t^{\beta}, \tag{1}$$

$$y_{t+1}^{\alpha}(i) = g(x_t^{\alpha}(i), y_t^{\alpha}(i)); \tag{2}$$

$$x_{t+1}^{\beta}(j) = (1-\mu) f(x_t^{\beta}(j), y_t^{\beta}(j)) + \mu \bar{X}_t^{\beta} + \epsilon \bar{X}_t^{\alpha}, \tag{3}$$

$$y_{t+1}^{\beta}(j) = g(x_t^{\beta}(j), y_t^{\beta}(j)), \tag{4}$$

where the functions $f(x, y)$ and $g(x, y)$ describe the local dynamics, and parameters μ and ϵ characterize the strength of the intra-population and inter-population coupling, respectively. The mean fields of populations α and β at time t are defined, respectively, as

$$\bar{X}_t^{\alpha} = \frac{1}{N^{\alpha}} \sum_{i=1}^{N^{\alpha}} x_t^{\alpha}(i), \tag{5}$$

$$\bar{X}_t^{\beta} = \frac{1}{N^{\beta}} \sum_{j=1}^{N^{\beta}} x_t^{\beta}(j). \tag{6}$$

Figure (1) illustrates the system of two interacting populations of dynamical elements Eqs. (1–4).

Synchronization states for each population can be characterized by the following asymptotic time averages, after discarding a number of transients τ,

$$\langle \sigma^{\alpha} \rangle = \frac{1}{T-\tau} \sum_{t=\tau}^{T} \sigma_t^{\alpha}, \tag{7}$$

$$\langle \sigma^{\beta} \rangle = \frac{1}{T-\tau} \sum_{t=\tau}^{T} \sigma_t^{\beta}, \tag{8}$$

$$\langle \delta \rangle = \frac{1}{T-\tau} \sum_{t=\tau}^{T} |\bar{X}_t^{\alpha} - \bar{X}_t^{\beta}|, \tag{9}$$

where the instantaneous standard deviations of the distribution of state variables are defined by

$$\sigma_t^{\alpha} = \left[\frac{1}{N^{\alpha}} \sum_{i=1}^{N^{\alpha}} (x_t^{\alpha}(i) - \bar{X}_t^{\alpha})^2 \right]^{1/2}, \tag{10}$$

$$\sigma_t^{\beta} = \left[\frac{1}{N^{\beta}} \sum_{j=1}^{N^{\beta}} (x_t^{\beta}(j) - \bar{X}_t^{\beta})^2 \right]^{1/2}. \tag{11}$$

A collective state of synchronization within population α $[\beta]$ for the system represented by Eqs. (1–2) and (3–4) takes place when $x_t^{\alpha[\beta]}(i) = x_t^{\alpha[\beta]}(k) = \bar{X}_t^{\alpha[\beta]}$ and $y_t^{\alpha[\beta]}(i) = y_t^{\alpha[\beta]}(k)$, $\forall i, k \in \alpha[\beta]$, sustained in time. Thus, a complete state of synchronization in population α is characterized by the condition $\langle \sigma^{\alpha} \rangle = 0$, and similarly, population β is synchronized when $\langle \sigma^{\beta} \rangle = 0$. In numerical simulations, we set the criterion $\langle \sigma^{\alpha[\beta]} \rangle < 10^{-7}$ for synchronization of a population.

Different collective states of synchronization can be defined in the system Eqs. (1–4):

1. Complete synchronization (CS): When all elements within each population are synchronized with each other and with the elements of the other population. That is, $\langle \sigma^{\alpha} \rangle = 0$, $\langle \sigma^{\beta} \rangle = 0$, and $\langle \delta \rangle = 0$.
2. Generalized synchronization (GS): When the elements within each population are synchronized but not with the elements of the other population [51]. That is, $\langle \sigma^{\alpha} \rangle = 0$ and $\langle \sigma^{\beta} \rangle = 0$, but $\langle \delta \rangle \neq 0$.
3. Chimera state (Q): When the elements in one population are synchronized but the elements in the other population are not. That is, $\langle \sigma^{\alpha} \rangle = 0$, $\langle \sigma^{\beta} \rangle \neq 0$, or vice versa, and $\langle \delta \rangle \neq 0$.
4. Desynchronization (D): None of the populations exhibits synchronization. This means, $\langle \sigma^{\alpha} \rangle \neq 0$ and $\langle \sigma^{\beta} \rangle \neq 0$.

We consider the two-dimensional map proposed by Rulkov [52] as local neural dynamics, defined as

$$x_{t+1} = h(x_t, y_t), \tag{12}$$

$$y_{t+1} = y_t - \upsilon(x_t + 1) + \upsilon\gamma, \tag{13}$$

where x_t and y_t are the fast and slow variables. As for the two previous local maps, although these variables have not specific biological meaning, x_t can be interpreted as the

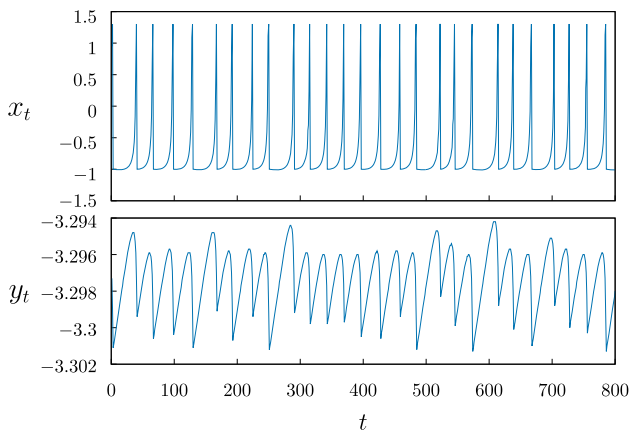

Fig. 2 Time series of a single Rulkov map, Eqs. (12–13), with parameters $\upsilon = 0.001$, $\varrho = 4.6$, and $\gamma = 0.225$

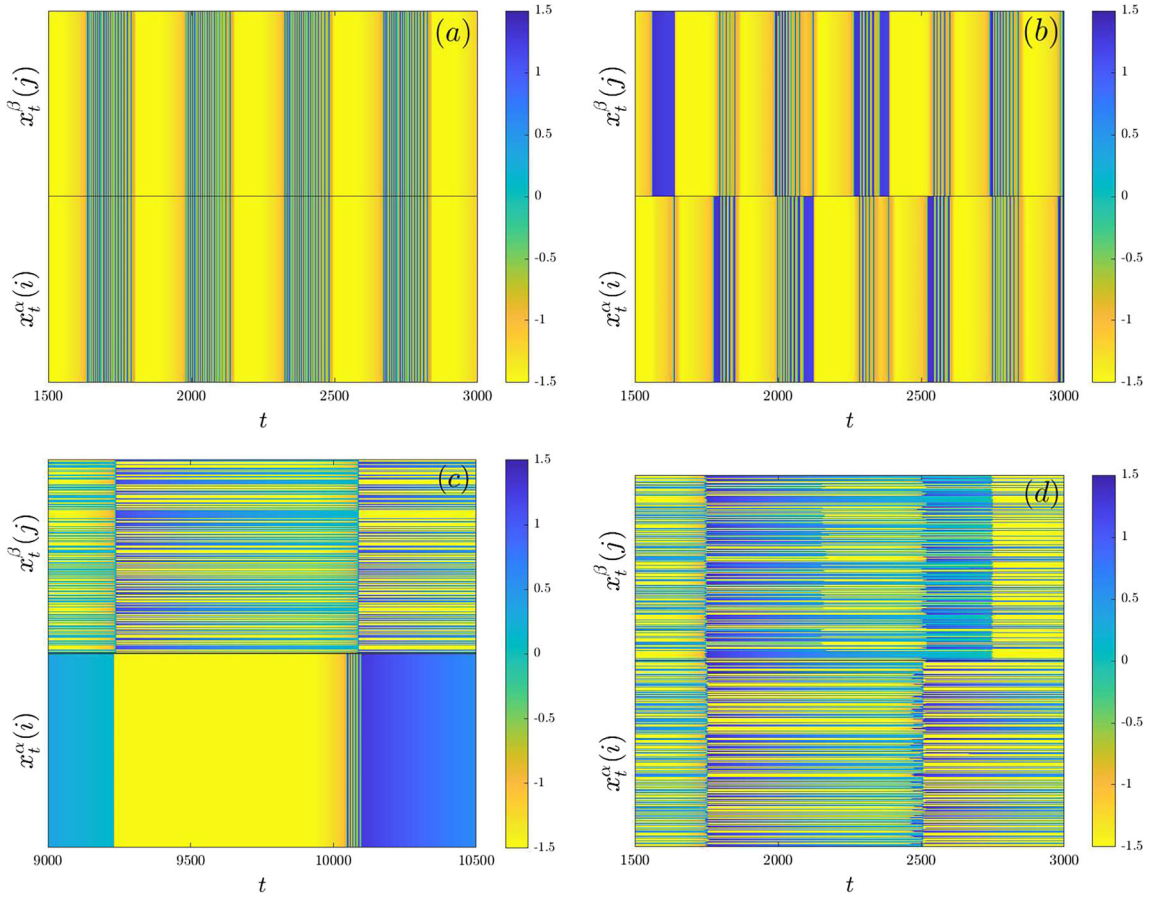

Fig. 3 Spatiotemporal patterns for the two-population model, Eqs. (1–4), with local Rulkov dynamics, Eqs. (12–13). Population sizes $N^\alpha = N^\beta = 400$. Fixed parameters $\upsilon = 0.001$, $\varrho = 4.6$, $\gamma = 0.225$. (**a**) Synchronization ($\langle\sigma^\alpha\rangle = \langle\sigma^\beta\rangle = 0$, $\langle\delta\rangle = 0$), $\mu = 0.08$ and $\epsilon = 0.04$. (**b**) Generalized synchronization ($\langle\sigma^\alpha\rangle = \langle\sigma^\beta\rangle = 0$, $\langle\delta\rangle \neq 0$), $\mu = 0.061$ and $\epsilon = 0.02$. (**c**) Chimera state ($\langle\sigma^\alpha\rangle \neq 0$ and $\langle\sigma^\beta\rangle = 0$), $\mu = 0.085$ and $\epsilon = 0.002$. (**d**) Desynchronized state ($\langle\sigma^\alpha\rangle \neq \langle\sigma^\beta\rangle \neq 0$), $\mu = 0.01$ and $\epsilon = 0.005$

transmembrane potential of a neuron, while y_t is a recovery or adaptation variable, where slow time evolution is given by small values of the parameter υ $(0 < \upsilon \ll 1)$.

To generate spiking and silent regimes, Eq. (12) employs a piecewise function $h(x, y)$ of the form

$$h(x,y) = \begin{cases} \varrho(1-x)^{-1} + y & \text{if} \quad x \leq 0, \\ \varrho + y & \text{if} \quad 0 < x < \varrho + y, \\ -1 & \text{if} \quad x \geq \varrho + y. \end{cases} \tag{14}$$

where γ and ϱ are control parameters that allow to select different regimes of temporal behavior of the model. Figure 2 shows the time evolution of the Rulkov map variables for parameter values $\upsilon = 0.001$, $\varrho = 4.6$, and $\gamma = 0.225$ which correspond to the chaotic spiking region, as reported in [53].

3 Synchronization and chimera states

Figure 3 shows the asymptotic evolution of the variables $x_t^\alpha(i)$, $\forall i \in \alpha$, and $x_t^\beta(j)$, $\forall j \in \beta$ for the two interacting population model, Eqs. (1–4), with Rulkov local dynamics, Eqs. (12–13), for different values of coupling parameters μ and ϵ. Spatiotemporal patterns for complete synchronization, generalized synchronization, chimera state, and desynchronization are shown.

Figure 4 shows the collective synchronization states of the two-population system, Eqs. (1–4), with local dynamics given by the Rulkov map, Eqs. (12–13), on the space of the coupling parameters (μ, ϵ). A complex structure is revealed in Fig. 4. Complete synchronization, generalized synchronization, disordered, and chimera states, characterized by the quantities $\langle\sigma^\alpha\rangle$, $\langle\sigma^\beta\rangle$, and $\langle\delta\rangle$, appear disperse over the parameter space (μ, ϵ).

To investigate the influence of asymmetry in the population sizes on the emergence of chimera states, we

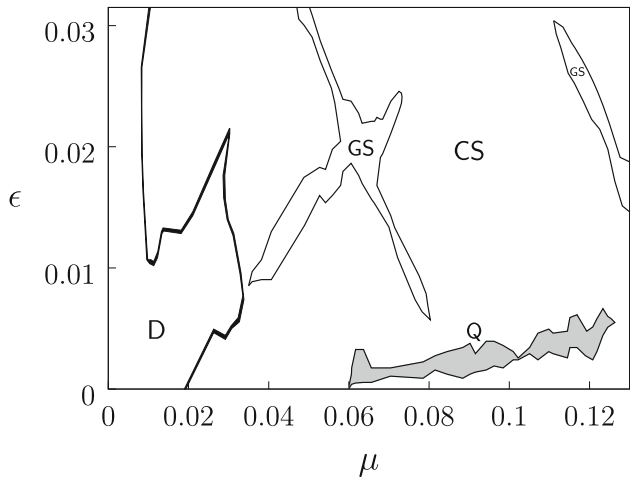

Fig. 4 Phase diagram on the space of parameters (μ, ϵ) for the two-population system, Eqs. (1–4), with local Rulkov dynamics, Eqs. (12–13). Fixed local parameters $\upsilon = 0.001$, $\varrho = 4.6$, and $\gamma = 0.225$. Population sizes $N^\alpha = N^\beta = 500$. For each data point, the quantities $\langle \sigma^\alpha \rangle$, $\langle \sigma^\beta \rangle$, and $\langle \delta \rangle$ that characterize the different synchronization states are calculated over 1000 iterations after discarding 3000 transients, and averaged over 100 realizations of random initial conditions for each population. Labels CS, GS, Q, and D indicate the regions where collective synchronization states occur. The region where chimera states (Q) appear is colored in gray

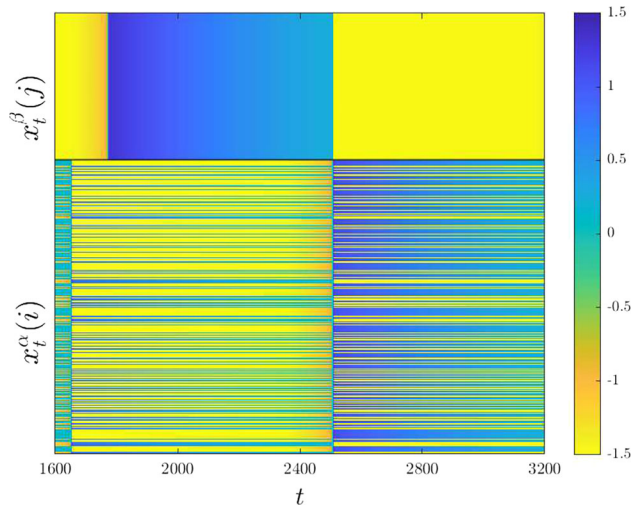

Fig. 5 Spatiotemporal pattern for a chimera state in the system, Eqs. (1–4), with different population sizes $N^\alpha \neq N^\beta$. Fixed parameters $\upsilon = 0.001$, $\varrho = 4.6$, and $\gamma = 0.225$. (**a**) Rulkov map for local dynamics, Eqs. (12–13), with fixed parameters $\upsilon = 0.001$, $\varrho = 4.6$, $\gamma = 0.225$, $\mu = 0.12$, $\epsilon = 0.0032$, $N^\alpha = 400$, and $N^\beta = 200$

performed simulations for different partitions of N^α and N^β. Figure 5 shows chimera patterns for two different partitions and for the two local map-based neurons considered in this article. The relative sizes of the populations do not affect the formation of chimeras with the reciprocal global coupling scheme of the system Eqs. (1–4).

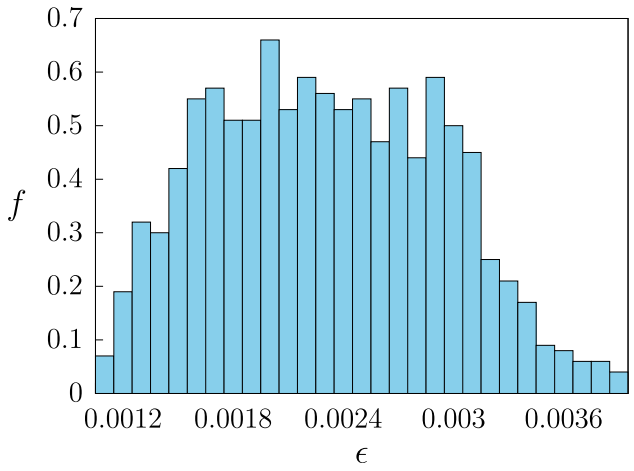

Fig. 6 Frequency f for the emergence of a chimera state as a function of ϵ and a fixed value of $\mu = 0.09$ for the interacting populations system Eqs. (1–4). The frequency for observing a chimera state is calculated over 100 realizations of random and uniformly distributed initial conditions for each value of ϵ. Local dynamics is given by Rulkov maps, Eqs. (12–13), with fixed parameters $\upsilon = 0.001$, $\varrho = 4.6$, and $\gamma = 0.225$. Population sizes are $N^\alpha = N^\beta = 500$

4 Information flow between neuron populations in chimera states

We note that chimera states are probabilistic, in the sense that their occurrence depends on initial conditions. Once formed, chimera states are stable. We calculate the frequency f for occurrence of a chimera state, with one population synchronized and the other incoherent, over 100 realizations of random initial conditions for given parameter values. Figure 6 shows the frequency f as a function of the inter-population coupling parameter ϵ, for a fixed value of μ. We have verified that the frequency to observe a chimera state does not change as the population sizes increase.

To elucidate the communication mechanisms between the neuron populations in a chimera state, we employ the information transfer introduced by Schreiber [43]. Consider two dynamical variables y_t and x_t interacting in a system. Then, the information transfer from y_t to x_t is defined as [43]

$$T_{y\to x} = \sum_{x_{t+1},x_t,y_t} p(x_{t+1},x_t,y_t) \log\left[\frac{p(x_{t+1},x_t,y_t)p(x_t)}{p(x_t,y_t)p(x_{t+1},x_t)}\right], \tag{15}$$

where $p(x_t)$ is the probability distribution of the time series x_t, $p(x_t, y_t)$ is the joint probability distribution of x_t and y_t, and so on. The quantity $T_{y\to x}$ measures the degree of dependence of x on y; i.e., the information required to represent the value x_{t+1} from the knowledge of y_t. Note that the information transfer is non-symmetrical, i.e., $T_{y\to x} \neq T_{x\to y}$. When the two variables are synchronized,

$x_t = y_t$; then, $T_{y\to x} = 0$. An advantage of the information transfer is that it does not require any knowledge of the dynamical system nor prior assumptions on data generation.

In our system, Eqs. (1–4), the two populations communicate through their respective mean fields. Thus, we consider the information transfer between the mean fields $\bar{X}_t^{\alpha}$ and $\bar{X}_t^{\beta}$ of populations α and β, respectively, when a chimera state is formed. We proceed as follows. For parameter values where a chimera state appears, after a transient time of 1500 iterations, we verify that a chimera state has formed and identify the synchronized and the desynchronized population with the labels S and D, respectively. Then, we take a time series of 1500 consecutive values for the mean fields of the synchronized and desynchronized populations, denoted by $\bar{X}_t^{S}$ and $\bar{X}_t^{D}$, respectively. From these data, we calculate the information transfers $T_{\bar{X}_t^S\to\bar{X}_t^D}$ and $T_{\bar{X}_t^D\to\bar{X}_t^S}$ by using the definition Eq. (15) [54].

Figure 7a shows the averaged quantities $T_{\bar{X}_t^D\to\bar{X}_t^S}$ and $T_{\bar{X}_t^S\to\bar{X}_t^D}$ as functions of the coupling ϵ in the region of parameters where chimera states arise. Figure 7a reveals that $T_{\bar{X}_t^D\to\bar{X}_t^S} > T_{\bar{X}_t^S\to\bar{X}_t^D}$, indicating a defined direction of the flow of information between the two neuron populations in chimera states, from the desynchronized population D to the synchronized one, S. We have also evaluated the statistical difference between the quantities $T_{\bar{X}_t^D\to\bar{X}_t^S}$ and $T_{\bar{X}_t^S\to\bar{X}_t^D}$ for different values of ϵ. To compare these quantities, we employ the Wilcoxon test which can be applied when the distribution of the difference between the two means of two samples cannot be assumed to be normally distributed. In Fig. 7b, we show the corresponding p-values as a function of ϵ. The dashed horizontal line marks the significance level 0.05. Very low p-values indicate that the differences between $T_{\bar{X}_t^D\to\bar{X}_t^S}$ and $T_{\bar{X}_t^S\to\bar{X}_t^D}$ are significant; therefore, Fig. 7b provides a statistical evidence that $T_{\bar{X}_t^D\to\bar{X}_t^S} > T_{\bar{X}_t^S\to\bar{X}_t^D}$ in the range of parameters where chimera states appear.

Thus, a functional directionality emerges in the system despite the structural symmetry of our model, i.e., population D acts as the driver of population S in a chimera state. This result is relevant in the context of epileptic seizures that have been related to chimera states in brain dynamics [26, 27]. It has been found that there is a significant coupling direction in the oscillations from the thalamus to the seizure zone during epileptic seizures [41].

We have verified that the formation of chimera states subsists as the sizes of the populations are increased by several orders of magnitude. In addition, we have investigated the influence of the size of the populations on the directionality of the flow of information in chimera states. Figure 8a shows the maximum frequency f_{max} for chimera

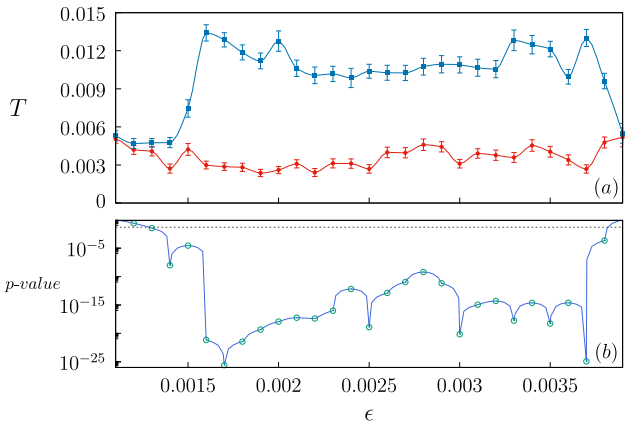

Fig. 7 (**a**) Averaged $T_{\bar{X}_t^D\to\bar{X}_t^S}$ (squares, blue line) and $T_{\bar{X}_t^S\to\bar{X}_t^D}$ (circles, red line) in chimera states as functions of the coupling parameter ϵ, for the system Eqs. (1–4) with fixed $\mu = 0.09$. Local dynamics is given by Rulkov maps, Eqs. (12–13), with fixed parameters $\upsilon = 0.001$, $\varrho = 4.6$, and $\gamma = 0.225$. Population sizes are $N^{\alpha} = N^{\beta} = 500$. Each data point of $T_{\bar{X}_t^D\to\bar{X}_t^S}$ and $T_{\bar{X}_t^S\to\bar{X}_t^D}$ is the average of 100 information transfer measures calculated over 100 realizations of initial conditions resulting in chimera states, where the synchronized and desynchronized populations S and D have been identified. Error bars represent the corresponding standard errors. (**b**) p-values obtained from the Wilcoxon test as a function of ϵ. The p-values characterize the statistical difference between the quantities $T_{\bar{X}_t^D\to\bar{X}_t^S}$ and $T_{\bar{X}_t^S\to\bar{X}_t^D}$. The dashed horizontal line signals the significance level 0.05 (color figure online)

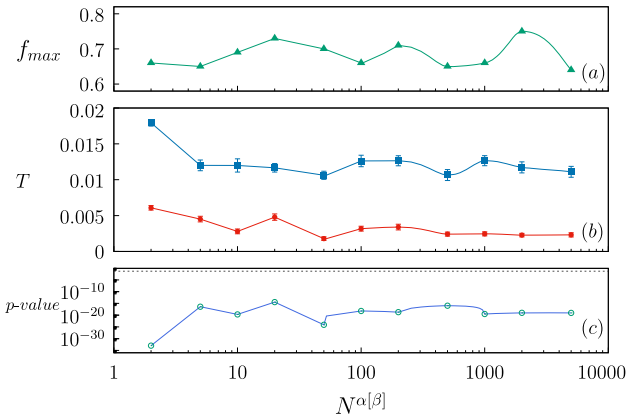

Fig. 8 (**a**) Maximum frequency for chimera states as function of the population size $N^{\alpha}(= N^{\beta})$ in the system Eqs. (1–4). (**b**) Averaged $T_{\bar{X}_t^D\to\bar{X}_t^S}$ (squares, blue line) and $T_{\bar{X}_t^S\to\bar{X}_t^D}$ (circles, red line) in chimera states as functions of the population size $N^{\alpha}(= N^{\beta})$ in the system Eqs. (1–4). Error bars represent the corresponding standard errors. (**c**) p-values obtained from the Wilcoxon test as a function of ϵ. The p-values characterize the statistical difference between the quantities $T_{\bar{X}_t^D\to\bar{X}_t^S}$ and $T_{\bar{X}_t^S\to\bar{X}_t^D}$. The dashed horizontal line signals the significance level 0.05. Each data point on (**a**) and (**b**) corresponds to parameters (μ, ϵ) where a chimera state has maximum frequency to occur. Local dynamics is given by Rulkov maps, Eqs. (12–13), with fixed parameters $\upsilon = 0.001$, $\varrho = 4.6$, and $\gamma = 0.225$ (color figure online)

states as a function of the population size $N^{\alpha}(=N^{\beta})$. For each population size, we explore values (μ, ϵ) for which chimera state arises with a frequency calculated over 100 realizations of initial conditions. Then, we determine f_{max} as the maximum value of these frequencies.

In Fig. 8b, for each population size $N^{\alpha}(=N^{\beta})$ and its corresponding parameters (μ, ϵ) for which the frequency of finding a chimera state is maximum, we calculate the averaged $T_{\bar{X}_t^D \to \bar{X}_t^S}$ and $T_{\bar{X}_t^S \to \bar{X}_t^D}$ by proceeding similarly as in Fig. 7. The result $T_{\bar{X}_t^D \to \bar{X}_t^S} > T_{\bar{X}_t^S \to \bar{X}_t^D}$ persists independently of the system size. We have calculated the p-values obtained from the Wilcoxon test between the quantities $T_{\bar{X}_t^D \to \bar{X}_t^S}$ and $T_{\bar{X}_t^S \to \bar{X}_t^D}$ from Fig. 8b. Figure 8c shows the corresponding p-values as a function of ϵ; they are much smaller than the significance level of 0.05. We note that the predominant direction of the information flow, from the desynchronized to the synchronized population, occurs even for the smallest possible populations of neurons $(N^{\alpha} = N^{\beta} = 2)$. We have verified that the result $T_{\bar{X}_t^D \to \bar{X}_t^S} > T_{\bar{X}_t^S \to \bar{X}_t^D}$ prevails if different population partitions are employed.

5 Conclusions

Coupled-map network models are computationally efficient, conceptually simple, and require few ingredients to study a variety of spatiotemporal processes, including synchronization phenomena, in complex systems and brain dynamics. In this article, we have investigated a system of two interacting populations of coupled maps subject to reciprocal global interactions, where the local units in each population exhibit neuron-like dynamics. We have focused on parameter values where the local maps exhibit chaotic spiking behavior. It has been found that chaotic dynamics in neurons leads to a greater diversity of responses that are relevant for neural computations [55].

We have characterized four collective synchronization states emerging in the system: (i) complete synchronization, where the populations are synchronized to each other, (ii) generalized synchronization, where each population is synchronized, but no to the other, (iii) chimera state, where one population is synchronized and the other remains incoherent, and (iv) desynchronization, where both populations are desynchronized.

Chimera states are probabilistic in the sense that their occurrence depends on initial conditions. On the parameter regions where the chimera states arise, the dynamics of the two-population system is multistable; i.e., several attractors coexist for the same parameter values. This behavior is typical of phase transition regions in dynamical systems. Chimeras represent an intermediate state between ordered and disordered phases.

We have found a well-defined direction of the flow of information in chimera states, from the desynchronized neuron population to the synchronized one. This result is independent of the population sizes or population partitions. The incoherent population functions as a driver of the coherent neuron population in a chimera state. This finding is consistent with the previous reports where a measure of transfer entropy, applied to epileptic electrocorticography data, shows a significant coupling direction from the anterior nucleus of thalamus to the synchronized seizure onset zone during seizures [41].

Although our results are obtained for specific neuron-map local dynamics, we expect that the drive–response causal relationship between the desynchronized and synchonized subsets persists for chimera states arising in general dynamical networks.

Models such as the presented here, where specific coupling parameters give rise to synchronization and chimera states, can provide insight to study phenomena such as unihemispheric sleep and brain disorders associated to alterations in the neural synchrony activity within and across brain areas [56]. Neurological disorders, such as epilepsy, Alzheimer's and Parkinson's disease, and autism, have been related to abnormal neural synchronization patterns [57–61].

Map-based neuron models are gaining recognition in the field of neuroscience, where they have been implemented in several studies [62–64]. Although the two-population model considered here is not specific in terms of biological plausibility, it yields the emergence of rich collective behavior that can be a useful tool in computational neuroscience. Future extensions of the two interacting population model proposed here should include the investigation of time delays, heterogeneity in the local dynamics, different connectivity networks, the similarity of collective states in driven and in autonomous systems, and the influence of external inputs.

Data availability This is a theoretical and computational work. There is no experimental or statistical data repository associated with this manuscript. The authors have elaborated the computer code employed in the numerical calculations, and it can be shared with interested researchers upon request.

Declarations

Conflict of interest The authors declare that they have no known competing financial interests or personal relationships that could have appeared to influence the work reported in this paper.

References

1. Montbrió E, Kurths J, Blasius B (2004) Synchronization of two interacting populations of oscillators. Phys Rev E 70(5):056125
2. Abrams DM, Mirollo R, Strogatz SH, Wiley DA (2008) Solvable model for chimera states of coupled oscillators. Phys Rev Lett 101(8):084103
3. Goel NS, Maitra SC, Montroll EW (1971) On the volterra and other nonlinear models of interacting populations. Rev Mod Phys 43(2):231
4. Gomatam J (1974) A new model for interacting populations. Bull Math Biol 36:347–353
5. Patriarca M, Leppänen T (2004) Modeling language competition. Physica A 338(1–2):296–299
6. Stefanescu RA, Jirsa VK (2008) A low dimensional description of globally coupled heterogeneous neural networks of excitatory and inhibitory neurons. PLoS Comput Biol 4(11):1000219
7. Maslennikov OV, Nekorkin VI (2014) Modular networks with delayed coupling: synchronization and frequency control. Phys Rev E 90(1):012901
8. Cardanobile S, Rotter S (2011) Emergent properties of interacting populations of spiking neurons. Front Comput Neurosci 5:59
9. Magyar A, Collins J (2015) Two-population model for medial temporal lobe neurons: the vast majority are almost silent. Phys Rev E 92(1):012712
10. Bibbig A, Traub RD, Whittington MA (2002) Long-range synchronization of γ and β oscillations and the plasticity of excitatory and inhibitory synapses: a network model. J Neurophysiol 88(4):1634–1654
11. Battaglia D, Witt A, Wolf F, Geisel T (2012) Dynamic effective connectivity of inter-areal brain circuits. PLoS Comput Biol 8(3):1002438
12. Barardi A, Sancristóbal B, Garcia-Ojalvo J (2014) Phase-coherence transitions and communication in the gamma range between delay-coupled neuronal populations. PLoS Comput Biol 10(7):1003723
13. Kuramoto Y, Battogtokh D (2002) Coexistence of coherence and incoherence in nonlocally coupled phase oscillators. Nonlinear Phenomena Compl Syst 5:380
14. Abrams DM, Strogatz SH (2004) Chimera states for coupled oscillators. Phys Rev Lett 93(17):174102
15. Panaggio MJ, Abrams DM (2015) Chimera states: coexistence of coherence and incoherence in networks of coupled oscillators. Nonlinearity 28(3):67
16. Zakharova A (2020) Chimera patterns in networks. Springer
17. Laing CR (2010) Chimeras in networks of planar oscillators. Phys Rev E 81(6):066221
18. Omelchenko I, Maistrenko Y, Hövel P, Schöll E (2011) Loss of coherence in dynamical networks: spatial chaos and chimera states. Phys Rev Lett 106(23):234102
19. Martens EA, Bick C, Panaggio MJ (2016) Chimera states in two populations with heterogeneous phase-lag. Chaos: An Interdisc J Nonlinear Sci 26(9)
20. Premalatha K, Chandrasekar V, Senthilvelan M, Lakshmanan M (2017) Chimeralike states in two distinct groups of identical populations of coupled stuart-landau oscillators. Phys Rev E 95(2):022208
21. González-Avella JC, Cosenza MG, San Miguel M (2014) Localized coherence in two interacting populations of social agents. Physica A 399:24–30
22. Martens EA, Thutupalli S, Fourriere A, Hallatschek O (2013) Chimera states in mechanical oscillator networks. Proc Nat Acad Sci 110(26):10563–10567
23. Tinsley MR, Nkomo S, Showalter K (2012) Chimera and phase-cluster states in populations of coupled chemical oscillators. Nat Phys 8(9):662–665
24. Rattenborg NC, Amlaner CJ, Lima SL (2000) Behavioral, neurophysiological and evolutionary perspectives on unihemispheric sleep. Neurosci Biobehav Rev 24(8):817–842
25. Lesku JA, Martinez-Gonzalez D, Rattenborg NC (2009) Phylogeny and ontogeny of sleep. The Neurosci Sleep 61:70
26. Lainscsek C, Rungratsameetaweemana N, Cash SS, Sejnowski TJ (2019) Cortical chimera states predict epileptic seizures. Chaos: An Interdisc J Nonlinear Sci 29(12):121106
27. Andrzejak RG, Rummel C, Mormann F, Schindler K (2016) All together now: analogies between chimera state collapses and epileptic seizures. Sci Rep 6(1):23000
28. Kang L, Tian C, Huo S, Liu Z (2019) A two-layered brain network model and its chimera state. Sci Rep 9(1):14389
29. Li X, Xu T, Li J (2019) Synchronization and chimera states in a multilayer neuronal network with unidirectional interlayer links. The Eur Phys J Spec Top 228:2419–2427
30. Glaze TA, Lewis S, Bahar S (2016) Chimera states in a hodgkin-huxley model of thermally sensitive neurons. Chaos: An Interdisc J Nonlinear Sci 26(8):083119
31. Hizanidis J, Kouvaris NE, Zamora-López G, Díaz-Guilera A, Antonopoulos CG (2016) Chimera-like states in modular neural networks. Sci Rep 6(1):19845
32. Bera BK, Ghosh D, Lakshmanan M (2016) Chimera states in bursting neurons. Phys Rev E 93(1):012205
33. Glaze TA, Bahar S (2021) Neural synchronization, chimera states and sleep asymmetry. Front Netw Physiol 1:734332
34. Omelchenko I, Provata A, Hizanidis J, Schöll E, Hövel P (2015) Robustness of chimera states for coupled fitzhugh-nagumo oscillators. Phys Rev E 91(2):022917
35. Essaki Arumugam EM, Spano ML (2015) A chimeric path to neuronal synchronization. Chaos: An Interdisc J Nonlinear Sci 25(1):013107
36. Rybalova E, Bukh A, Strelkova G, Anishchenko V (2019) Spiral and target wave chimeras in a 2d lattice of map-based neuron models. Chaos: An Interdisc J Nonlinear Sci 29(10)
37. Mehrabbeik M, Parastesh F, Ramadoss J, Rajagopal K, Namazi H, Jafari S (2021) Synchronization and chimera states in the network of electrochemically coupled memristive rulkov neuron maps. Math Biosci Eng 18(6):9394–9409
38. Bossomaier T, Barnett L, Harré M, Lizier JT (2016) An introduction to transfer entropy: information flow in complex systems. Springer International Publishing
39. Cisneros L, Jiménez J, Cosenza MG, Parravano A (2002) Information transfer and nontrivial collective behavior in chaotic coupled map networks. Phys Rev E 65(4):045204
40. Wibral M, Vicente R, Lindner M (2014) Directed information measures in neuroscience. Springer, Berlin
41. Li Z, Li S, Yu T, Li X (2020) Measuring the coupling direction between neural oscillations with weighted symbolic transfer entropy. Entropy 22(12):1442

42. Ursino M, Ricci G, Magosso E (2020) Transfer entropy as a measure of brain connectivity: a critical analysis with the help of neural mass models. Front Comput Neurosci 14:45
43. Schreiber T (2000) Measuring information transfer. Phys Rev Lett 85:461
44. Deschle N, Daffertshofer A, Battaglia D, Martens EA (2019) Directed flow of information in chimera states. Front Appl Math Stat 5:28
45. Kaneko K (1984) Period-doubling of kink-antikink patterns, quasiperiodicity in antiferro-like structures and spatial intermittency in coupled logistic lattice: towards a prelude of a field theory of chaos. Progress Theoret Phys 72(3):480–486
46. Waller I, Kapral R (1984) Spatial and temporal structure in systems of coupled nonlinear oscillators. Phys Rev A 30(4):2047
47. Kaneko K (1993) Theory and applications of coupled map lattices. Theory and Applications, Nonlinear Science
48. Cosenza MG, Kapral R (1992) Coupled maps on fractal lattices. Phys Rev A 46(4):1850
49. Naze S, Bernard C, Jirsa V (2015) Computational modeling of seizure dynamics using coupled neuronal networks: factors shaping epileptiform activity. PLoS Comput Biol 11(5):1004209
50. Breakspear M, Jirsa VK (2007) Neuronal dynamics and brain connectivity. In: Handbook of Brain Connectivity, 3–64. Springer
51. Alvarez-Llamoza O, Cosenza MG (2008) Generalized synchronization of chaos in autonomous systems. Phys Rev E 78(4):046216
52. Rulkov NF (2002) Modeling of spiking-bursting neural behavior using two-dimensional map. Phys Rev E 65(4):041922
53. Shilnikov AL, Rulkov NF (2003) Origin of chaos in a two-dimensional map modeling spiking-bursting neural activity. Int J Bifurc Chaos 13(11):3325–3340
54. Behrendt S, Dimpfl T, Peter FJ, Zimmermann DJ (2019) Rtransferentropy-quantifying information flow between different time series using effective transfer entropy. SoftwareX 10:100265
55. Rasmussen R, Jensen MH, Heltberg ML (2017) Chaotic dynamics mediate brain state transitions, driven by changes in extracellular ion concentrations. Cell Syst 5(6):591–603
56. Wang Z, Liu Z (2020) A brief review of chimera state in empirical brain networks. Front Physiol 11:724
57. Uhlhaas PJ, Singer W (2006) Neural synchrony in brain disorders: relevance for cognitive dysfunctions and pathophysiology. Neuron 52(1):155–168
58. Delbeuck X, Linden M, Collette F (2003) Alzheimer'disease as a disconnection syndrome? Neuropsychol Rev 13:79–92
59. Babiloni C, Del Percio C, Lizio R, Noce G, Cordone S, Lopez S, Soricelli A, Ferri R, Pascarelli MT, Nobili F et al (2017) Abnormalities of cortical neural synchronization mechanisms in subjects with mild cognitive impairment due to alzheimer's and parkinson's diseases: an eeg study. J Alzheimers Dis 59(1):339–358
60. Jiruska P, De Curtis M, Jefferys JG, Schevon CA, Schiff SJ, Schindler K (2013) Synchronization and desynchronization in epilepsy: controversies and hypotheses. The J Physiol 591(4):787–797
61. Dinstein I, Pierce K, Eyler L, Solso S, Malach R, Behrmann M, Courchesne E (2011) Disrupted neural synchronization in toddlers with autism. Neuron 70(6):1218–1225
62. Nowotny T, Huerta R, Abarbanel HD, Rabinovich MI (2005) Self-organization in the olfactory system: one shot odor recognition in insects. Biol Cybern 93:436–446
63. Yu L, De Mazancourt M, Hess A, Ashadi FR, Klein I, Mal H, Courbage M, Mangin L (2016) Functional connectivity and information flow of the respiratory neural network in chronic obstructive pulmonary disease. Hum Brain Mapp 37(8):2736–2754
64. Sayari E, Gabrick EC, Borges FS, Cruziniani FE, Protachevicz PR, Iarosz KC, Szezech JD, Batista AM (2023) Analyzing bursting synchronization in structural connectivity matrix of a human brain under external pulsed currents. Chaos: An Interdisc J Nonlinear Sci 33(3)